Swansea University
Prifysgol Abertawe

Cronfa
Setting Research Free

Cronfa - Swansea University Open Access Repository

This is an author produced version of a paper published in :
Materials Science and Engineering: A

Cronfa URL for this paper:
http://cronfa.swan.ac.uk/Record/cronfa15000

Paper:
Whittaker, M., Wilshire, B. & Brear, J. (2013). Creep Fracture of the Centrifugally-Cast Superaustenitic Steels, HK40 and HP40. *Materials Science and Engineering: A*

http://dx.doi.org/10.1016/j.msea.2013.05.041

This article is brought to you by Swansea University. Any person downloading material is agreeing to abide by the terms of the repository licence. Authors are personally responsible for adhering to publisher restrictions or conditions. When uploading content they are required to comply with their publisher agreement and the SHERPA RoMEO database to judge whether or not it is copyright safe to add this version of the paper to this repository.
http://www.swansea.ac.uk/iss/researchsupport/cronfa-support/

Creep Fracture of the Centrifugally-Cast Superaustenitic Steels, HK40 and HP40

M Whittaker[1], B Wilshire[1], J Brear[2]

[1] Materials Research Centre, College of Engineering, Swansea University, Singleton Park, Swansea. SA2 8PP

[2] Stress Engineering Services (Europe) Ltd, Llanelli, SA14 7BP, UK

Corresponding author: M Whittaker, Materials Research Centre, College of Engineering, Swansea University, Singleton Park, Swansea. SA2 8PP +44 1792 295573 (Tel) +44 1792 295693 (Fax). m.t.whittaker@swansea.ac.uk (e-mail)

Abstract

Practical experience of creep failure of components in service are discussed in relation to the creep rupture properties of HK40 (25Cr-20Ni-0.4C) and HP40 (25Cr-35Ni), which are considered using traditional and new data analysis procedures. The new approach is shown to offer not only a sensible mechanistic interpretation of the observed behaviour patterns but also a reasonable method for predicting long-term fracture strengths by extrapolation of short term creep life values.

Keywords: Creep, Failure Modes, Creep life prediction, HK40, HP40

Introduction

There are many situations that require weldable, heat-resisting steels having good creep strength, together with oxidation and carburisation resistance at temperatures up to and exceeding 1000°C. Suitable steels are typically 'super-austenitics' with over 20% each of chromium and nickel. These are invariably supplied either as centrifugal castings for tubes or as static castings for applications such as retorts and supports, hangers and other parts for process and heat-treatment furnaces.

Typical examples are HK40 (25%Cr-20%Ni-0.4%C) and HP40 (25%Cr-35%Ni), which are included in such specifications as ASTM A297. Later developments, such as the niobium modified HP steels and the 35%Cr-45%Ni materials, are proprietary alloys with subtle differences between the variants supplied by different foundries. Although these newer grades are not yet consistently standardised, the continuing aim of alloy development is to maximise the creep strength and ductility, simultaneously improving the resistance to corrosion in oxidising, sulphurous and reducing furnace environments, plus the resistance to carburising process fluids. Some manufacturers also produce modified alloys with controlled additions of silicon to improve resistance to sigma phase formation.

HK40 and HP40 have been selected for the present study because they may be considered generic for these types of alloy and, being covered by compatible national standards, have a large amount of mechanical property data in the public domain. It should be noted that the majority of test data underlying the standards has been obtained on centrifugally-cast tubes, rather than on static castings. These steels may be supplied as-cast or aged.

Perhaps the most comprehensive data sets are those made available by the National Institute for Materials Science (NIMS), Japan [1, 2]. These documents provide both tensile properties and stress rupture measurements up to around 100,000h for a range of individual heats. In addition, information is supplied on the manufacturing processes and compositions, also presenting micrographs of samples prior to and after creep fracture.

Both as-cast steels are fully austenitic, having microstructures consistent with the casting process. A typical centrifugally-cast tube has at least 75% of the wall consisting of radiating, columnar grains with a pronounced dendritic structure and an inner-surface zone of equiaxed material, formed as the cooling rate rises at the end of the pour. With thermal exposure, secondary carbide precipitation becomes very dense (Fig.1). The increased alloy content in HP40 improves the long term stability of these carbides and is reflected in the better tensile and rupture strengths at the higher temperatures (Fig.2).

In highly carburising environments, such as steam-cracker tubes for ethylene production, carburisation usually dominates failure but, in all other applications [3], life is governed by creep processes (Fig. 3). At service temperatures and stresses, the older HK40 casts seldom achieved more than 1% creep ductility, whereas newer, cleaner examples can show around 5% or more, as does HP40. Deformation appears to occur predominantly in grain-boundary regions, reflecting the lower precipitate density, so that creep cavitation is common. The distributions of creep strain, cavity density and eventual cracking through a component then reflect the complex mechanical and thermal stress fields commonly encountered during service, with these variables also influenced by the differences in properties between the columnar and equiaxed structures. Hence, because creep failure often limits component life, a new methodology for rationalisation and extrapolation of creep properties [4-8] is now evaluated in relation to traditional methods for estimation of 100,000h rupture strengths, using the NIMS stress rupture data for these microstructurally-complex steels [1,2].

Experimental observations

For over half a century, the creep and creep fracture properties of metals and alloys have been described through the variations of the minimum creep rate ($\dot{\varepsilon}_m$) and the creep rupture life (t_f) with stress (σ) and temperature (T) using power law equations of the form

$$M/t_f = \dot{\varepsilon}_m = A\sigma^n \exp(-Q_C / RT) \qquad (1)$$

where R=8.314Jmol^{-1}K^{-1}. Unfortunately, the parameters (M and A), the stress exponent (n) and the apparent activation energy for creep (Q_c) vary as the stress/temperature conditions are altered. As evident from Fig.2(a), n decreases from around 4.6 at 1073K to about n=3.6 at 1273K over stress ranges giving creep lives up to 100,000h, with Q_c ranging from 250 to 300kJmol^{-1}.

For HK40 [1] and HP40 [2], the NIMS data sheets record the rupture life (t_f), the creep ductility (ε_f) and the reduction in area at fracture (RoA), whereas properties such as the minimum creep rate ($\dot{\varepsilon}_m$) and the times to various creep strains (t_ε) were not reported. Clearly, from Fig.2, the creep rupture strength of HP40 is marginally greater than that of HK40. However, the ε_f value (as well as the RoA properties) rises as the applied stress is reduced at temperatures approaching 1273K and above with HK40, whereas these values are fairly constant at around 15% as the rupture times increase towards 100,000h with HP40 (Fig.4).

The observation that n and Q_c vary as the test conditions change means that eqn.(1) cannot be used to predict 100,000h stress rupture data from measurements of the short term t_f values. Instead, the NIMS results used various parametric methods, such as the Larson-Miller method [9] with HK40 [1] and the Manson-Haferd relationship [10] with HP40 [2]. Using all of the NIMS results [1,2], the stresses giving creep lives of 100,000h using these approaches are listed in Table I.

Without recourse to traditional parametric curve fitting procedures, the stress rupture data at different temperatures can be superimposed onto 'master curves' simply by normalizing σ through the ultimate tensile strength (σ_{TS}) determined from high-strain-rate (10^{-3}s^{-1}) tests at the creep temperatures for each batch of material studied [4-10]. Adopting this approach, so that the data sets can be described over the full stress range from $\sigma/\sigma_{TS} \rightarrow 1$ to $\sigma/\sigma_{TS} \rightarrow 0$, eqn.(1) becomes

$$M/t_f = \dot{\varepsilon}_m = A^*\left(\sigma / \sigma_{TS}\right)^n \exp(-Q_C^* / RT) \qquad (2)$$

where $A^* \neq A$, while Q_c^* is obtained from the temperature dependencies of t_f at constant (σ/σ_{TS}) rather than Q_c which is calculated from the temperature dependencies of t_f at constant σ. In this way, as evident from Fig.5, the t_f data sets for HK40 [1] and HP40 [2] are superimposed with Q_c^*=100kJmol^{-1}.

It should be noted that reasonable extrapolations of UTS over the temperature range 1223-1373K have been enforced in HP40 since no data was available from NIMS. This extrapolation was based on the best fit line of the UTS as a function of temperature in both HK40 and HP40, and assumes minimal microstructural evolution in high-strain-rate tensile tests. The UTS values are consistent with extrapolation of short term creep tests towards zero time.

The value of Q_c*=100kJmol^{-1} is substantially smaller than the results for Q_c=250-300kJmol^{-1}, but replacing eqn.(1) with eqn.(2) does not eliminate the decreases in n value as the stress is lowered and the temperature is raised (Fig.5). Because this decrease in n value is unpredictable, eqn.(2) also fails to provide reliable long-term creep rupture strengths by analysis of short-term t_f data. For this reason, new extrapolation procedures have been devised recently [4-10] based on normalization of σ through σ_{TS}.

For a range of power plant steels [5-8], as well as various non-ferrous materials [4,11], the stress rupture properties are well described by the equation

$$(\sigma / \sigma_{TS}) = \exp\left\{-k_1\left[t_f . \exp\left(-Q_c^* / RT\right)\right]^u\right\} \qquad (3)$$

with similar relationships quantifying the stress and temperature dependencies of $\dot{\varepsilon}_m$ and t_ε. The coefficients in eqn.(3) are easily determined by plotting $\ln\left[t_f . \exp\left(-Q_c^* / RT\right)\right]$ as a function of ln [-ln (σ/σ_{TS})], with the present calculations of k_1 and u being based only on t_f values from tests with a maximum duration of 5000h (Table II). Despite the batch-to-batch scatter, the results can be represented by single straight lines, giving k_1=0.76 and u=0.15 for HK40 and k_1=0.78 and u=0.12 for HP40 (Fig.6). Incorporating these values into eqn.(3) then produces the sigmoidal 'master curves' shown for HK40 and HP40 in Fig.7. This procedure then satisfies the requirement that $t_f \rightarrow 0$ when $\sigma/\sigma_{TS} \rightarrow 1$, with inflections in the curves ensuring that $t_f \rightarrow \infty$ as $\sigma/\sigma_{TS} \rightarrow 0$. To assess this new methodology, the stresses giving creep lives of 100,000h are calculated using eqn.(3) and compared with the results obtained by NIMS when parametric approaches are adopted in Table I.

The log $t_f/(\sigma/\sigma_{TS})$ curves constructed using eqn.(3) appear to fit well with the measured stress rupture data (Fig.7). Even so, the 100,000h strengths predicted by applying eqn.(3) to results with t_f<5000h are lower than the values estimated by using the various parametric relationships to describe the full NIMS data sets (Table I). Yet, in several recent studies employing a range of parametric, numerical and computational procedures for creep data extrapolation, these techniques predicted creep rupture strengths higher than those found on conducting long-term tests. Consequently, it has been proposed that short-term t_f values should be discarded to avoid serious overestimation of 100,000h life properties [12,13], although no satisfactory procedures were suggested to decide on the results to be

ignored. For this reason, the predictions based on eqn.(3) appear very reasonable (Table I), except possibly the value of 4.3MPa expected for HK40 at 1000°C when the creep ductility increases very rapidly with decreasing stress at this temperature and above (Fig.4).

Discussion

With many steels selected for manufacture of large-scale components for power and petrochemical plant, using eqn.(3), the Q_c* value falls from around 300kJmol^{-1} to less than half of this value when σ is reduced from above to below σ_{PS}, where σ_{PS} is the proof stress of each batch of material at the creep temperature. When $\sigma>\sigma_{PS}$, the initial strain on loading (ε_0) has elastic and plastic components, whereas only elastic components are found when $\sigma<\sigma_{PS}$. Thus, creep is governed by the movement of new dislocations generated within the grains during the plastic component of the initial extension when $\sigma> \sigma_{PS}$, but by the movement of dislocations pre-existing in the material when $\sigma<\sigma_{PS}$. This is equivalent to stating that creep is governed largely by grain deformation when $\sigma>\sigma_{PS}$, but by grain boundary zone deformation when $\sigma<\sigma_{PS}$, where zone deformation consists of grain boundary sliding and associated deformation in regions of the grain adjacent to the boundaries. This interpretation is fully consistent with Q_c*=300kJmol^{-1} when grain deformation predominates, but with Q_c*=100kJmol^{-1} when grain boundary zone deformation is rate controlling, i.e. Q_c*=300kJmol^{-1} is the activation energy for lattice diffusion in the grains, whereas Q_c*=100kJmol^{-1} is expected when diffusion occurs within the boundary or along dislocations in regions adjacent to the boundaries in HK40 and HP40.

Although no information on the magnitude of the initial extension (ε_0) with changing stress levels was recorded by NIMS for HK40 and HP40, in both cases, the applied stresses were always well below σ_{PS}, so creep would be controlled by grain boundary zone deformation. As a result of this zone boundary deformation, grain boundary cavities form and grow along the columnar grain boundaries (Fig.8), with cavity link up forming transgranular cracks which develop through the wall thickness of HK40 and HP40 tubes to cause low ductility failures in service (Fig.9). Even so, with HK40, the rapid increase in creep ductility with decreasing stress at 1000°C and above (Fig.4) may eventually limit the crack incidence as microstructure degradation reduces the creep strength to allow deformation of the boundary regions to limit cavity and crack formation.

Conclusions

In quantifying the long-term stress rupture properties obtained for two centrifugally-cast superaustenitic steels, HK40 (20Cr-20Ni) and HP40 (25Cr-35Ni) by the National Institute for

Materials Science (NIMS), Japan, new relationships describing the stress and temperature dependencies of the creep lives (t_f) are shown to offer theoretical and practical advantages over traditional data analysis procedures.

These new approaches rationalize the creep rupture properties by normalizing the applied stress (σ) through the proof stress (σ_{PS}) and the tensile strength (σ_{TS}) of each batch of material at the creep temperatures. Thus, with σ_{TS} being the highest stress which can be applied at the creep temperature, sigmoidal creep life/(σ/σ_{TS}) curves are produced, such that $t_f \rightarrow 0$ when $(\sigma/\sigma_{TS}) \rightarrow 1$, while $t_f \rightarrow \infty$ when $(\sigma/\sigma_{TS}) \rightarrow 0$.

When $\sigma > \sigma_{PS}$, previous research [4] has shown that creep occurs by the movement of new dislocations generated within the grains but, with HK40 and HP40, σ was always well below σ_{PS}, so creep occurs by the movement of pre-existing dislocations. Specifically, when $\sigma < \sigma_{PS}$, it is assumed that creep occurs by grain boundary zone deformation, i.e. grain boundary sliding and associated dislocation movement in regions of the grain adjacent to grain boundaries. This zone deformation results in the formation of cavities, leading to intergranular crack development along the columnar boundaries of HK40 and HP40, giving relatively low-ductility intergranular fracture.

In contrast to traditional methodologies, the new relationships also allow reasonable prediction of long-term rupture values by extrapolation of short-term data for HK40 and HP40 at 800 to 1000°C. Even so, the predicted lives may overestimate the long-term performance of HK40 when the creep ductility increases rapidly with decreasing applied stress at 1000°C and above.

References

1. NIMS Creep Data Sheet No 16B. Data sheets on the elevated temperatures properties of centrifugally-cast 25Cr-20Ni-0.4C steel tubes for use in reformer furnaces (SCH 22-CF).
2. NIMS Creep Data Sheet 38A Data sheets on the elevated temperature properties of centrifugally cast tubes and cast block of 25Cr-35Ni-0.4C steel for reformer furnaces (SCH 24).
3. J. Williamson, J.M. Brear. Fourth annual Ammonia and Urea Conf., ‘Asia 2000’, Singapore, June 2000.
4. B. Wilshire, A. Battenbough. Mater. Sci. Eng. A, 443A (2007) 156-166.
5. B. Wilshire, P.J. Scharning. Int. J. Press. Vessels and Piping. 85 (2008) 739-743.
6. B. Wilshire, P.J. Scharning. Mater. Sci. Tech. 24 (2008) 1-9.
7. M.T. Whittaker, B. Wilshire. Mat. Met. Trans. A. 44A (2013) 136-153.

8. B. Wilshire, P.J. Scharning. Int. Mater. Rev. 53 (2008) 91-104.
9. F.R. Larson, J. Miller. Trans ASME 74 (1952) 765-775.
10. S.S. Manson, A.M. Haferd. (1953) NASA. TN 2890.
11. Z.M. Abdallah, K.M. Perkins, S.J. Williams. Mat. Sci. Eng. A. 550 (2012) 176-182.
12. P.J. Ennis in 'Creep and Fracture in high-temperature components – design and life assessment issues' (ed. I.A. Shibli et al) London DesTech Publ. Inc. (2005) 279-287
13. K. Kimura in 'Creep and Fracture in high-temperature components – design and life assessment issues' (ed. I.A. Shibli et al) London DesTech Publ. Inc. (2005) 1008-1022.

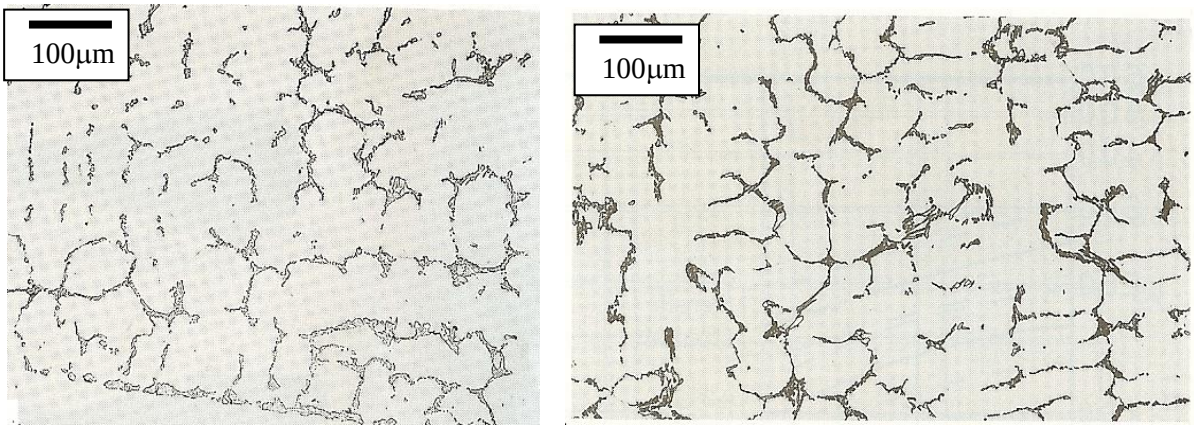

Figure 1. The microstructural appearances of the superaustenitic steels, (a) HK40 (b) HP40

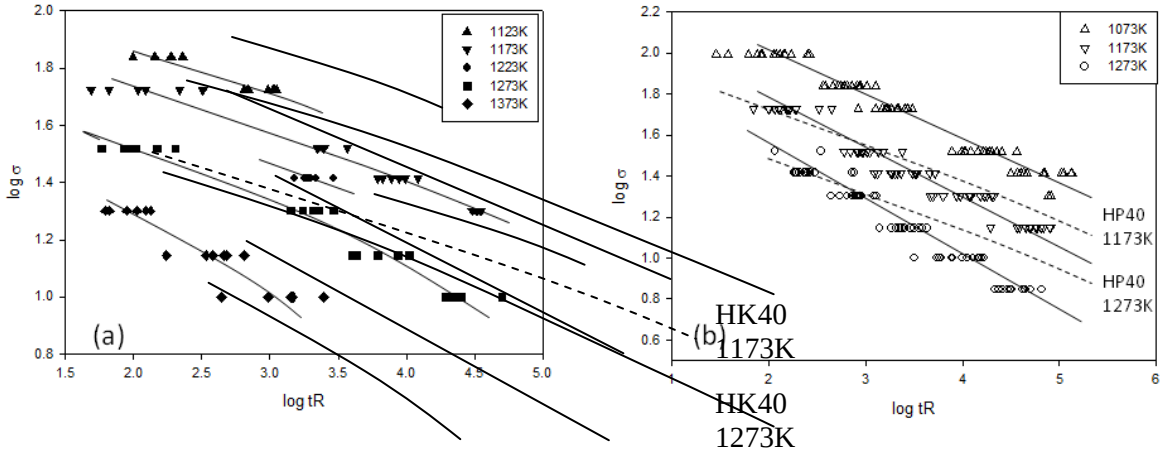

Figure 2. The multibatch properties of the superaustenitic steels, (a) HK40 [1] and (b) HP40 [2].

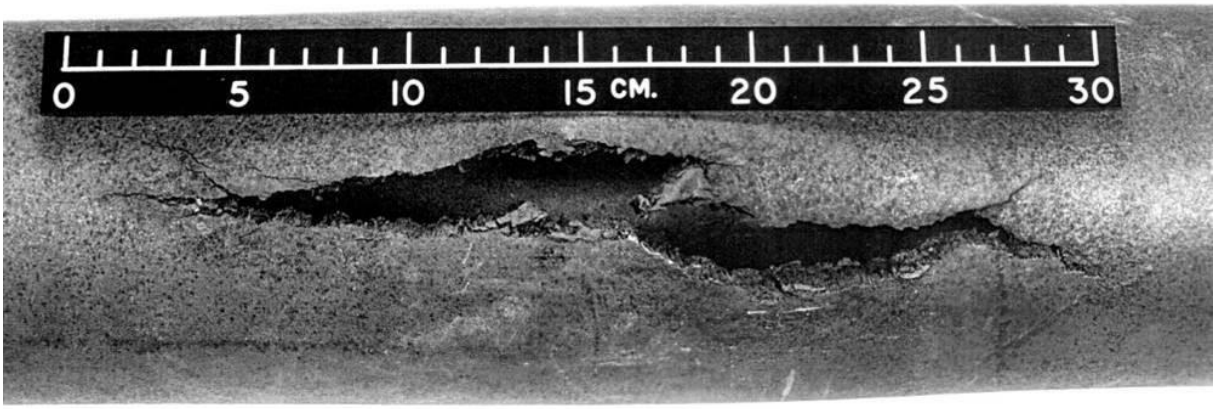

Figure 3. Creep failure of centrifugally-cast HK40 tube during service [3].

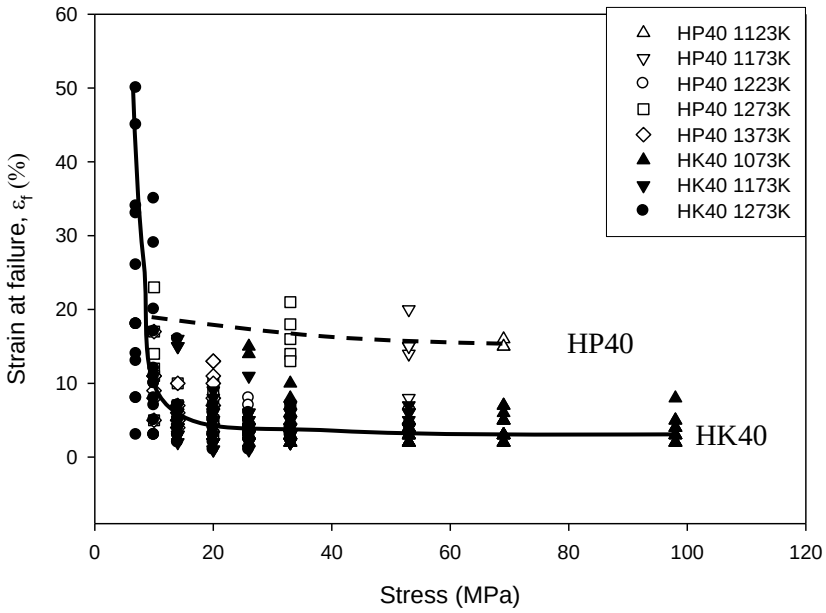

Figure 4. The stress dependences of the creep ductility (%) of centrifugally-cast tube steels, HK40 (closed symbols) and HP40 (open symbols).

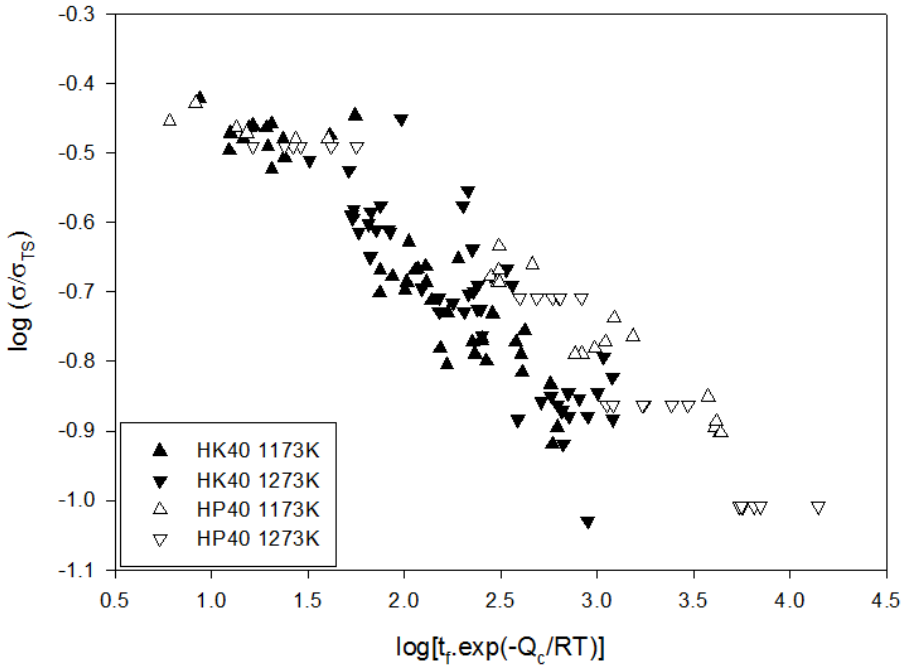

Figure 5: Multi-batch stress rupture data for the centrifugally-cast tube steels, HK40 (closed symbols) and HP40 (open symbols), superimposed at 1173 and 1273K using equation (2) with Q_c*=100kJmol^{-1}.

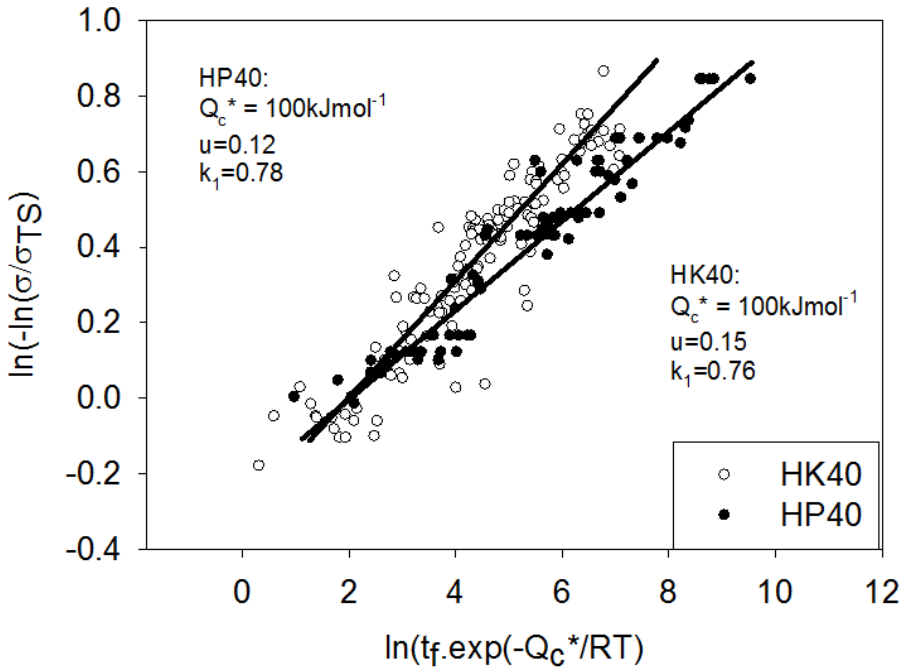

Figure 6: The variations in the temperature compensated creep life as a function of ln[-ln(σ/σ_{TS})] allowing computation of the k_1 and u values in equation (3), with Q_c*=100kJmol^{-1} for the centrifugally-cast tube steels, HK40 (open symbols) and HP40 (closed symbols).

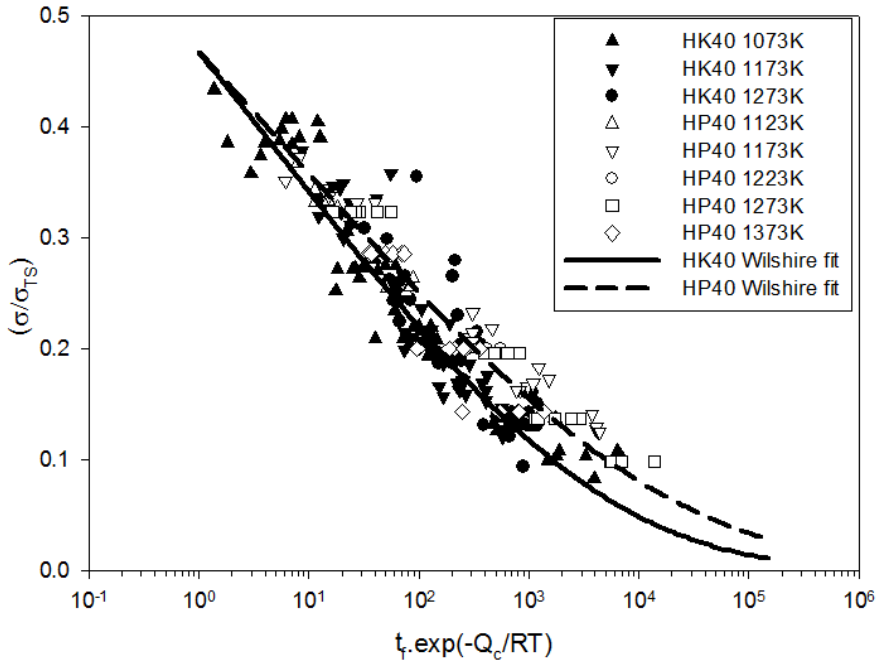

Figure 7: Analysing multi-batch stress rupture data from tests having a maximum duration of 5000h [1,2], the sigmoidal master curves constructed using equation (3) with Q_c*=100kJmol^{-1} (solid line) for HK40 (open symbols and solid line) and HP40 (full symbols and broken line) represent all creep life measurements at stresses causing failure in times up to 100,000h [1,2].

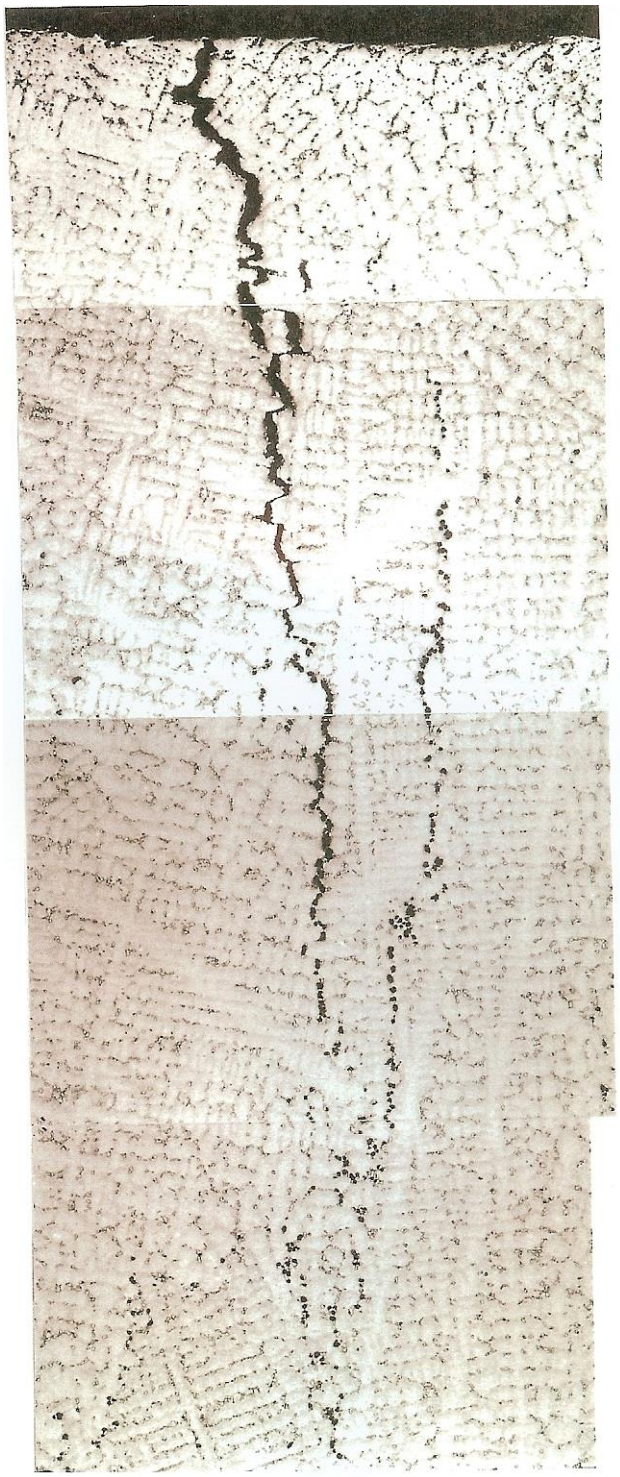

Figure 8: Cavity development along columnar grain boundaries during service of HK40 tube steel.

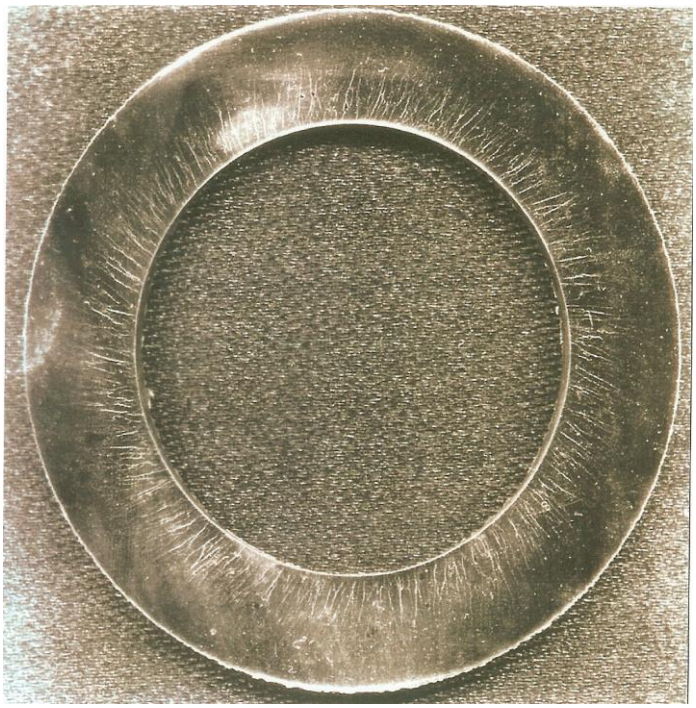

Figure 9: Creep crack development along the columnar grain boundaries of a centrifugally-cast HK40 tube during service.

Table I: Estimated stress for rupture in 100,000h (MPa)

Data analysis method	HK40			HP40		
	800°C	900°C	1000°C	800°C	900°C	1000°C
Eqn (3) for data <5000hr	19.8	9.1	4.3	13.6	10	6.9
NIMS data, Larson-Miller method	23.4	10.9	-	-	-	-
NIMS data, Manson-Haferd method	-	-	-	16	10	4.3

Table II: Values of k1 and u in equation (3), calculated from stress rupture data for creep lives up to 5000h, for centrifugally-cast HK40 [1] and HP40 [2] tube steels.

	HK40	HP40
u	0.14	0.12
k_1	0.66	0.87
Q_c^* (kJmol^{-1})	90	110